Identification of eroded sediment layer thickness and depth of Mahakam River at Tenggarong Bridge Area, Kutai Kartanegara East Kalimantan using Ground Penetrating Radar Method

IOP Conference Series: Earth and Environmental Science

Table of contents

Volume 279

2019

Previous issue Next issue

The International Conference on Geoscience 1–2 November 2018, Makassar, Indonesia

Accepted papers received: 23 April 2019
Published online: 05 September 2019

Open all abstracts

Preface

OPEN ACCESS 011001
Preface
+ Open abstract View article PDF

OPEN ACCESS 012040
Identification of eroded sediment layer thickness and depth of Mahakam River at Tenggarong Bridge Area, Kutai Kartanegara East Kalimantan using Ground Penetrating Radar Method
S Rasimeng, I Mandang and Suharno
− Close abstract View article PDF

GPR measurements of lines are two lines intersect under the bridge of Tenggarong (southwest to northeast) along the 377 meters (segment-1 Line04) and 457 meters (Line03) and the other is Southeast to Northwest along the 533 meters (segment-2 Line04) with a starting point It is located on the side of the Mahakam River (Southern) to the West of Kumala island. and there is one track in this area, which is to the northeast to the southwest along the south side of the Mahakam River (Line02) with the length of line is 780 meters. This research used the AKULA-9000C, 100 MHz antenna frequencies, and in time mode. The purpose of this research is to know the depth of the bottom of the Mahakam River, and the thickness of sediments eroded around the bridge of Tenggarong. GPR data processing using the ReflexW software ver. 8.5 through static correction, subtract-mean (dewow) filter, gain, background removal, band-pass filters, and fk-filter. To convert two-way time of electromagnetic wave propagation data to depth units, we use velocity adaptation methods by selecting velocity value each layer anomaly. Cross sections of the line from line02 and Line03 showed that the average thickness of the layer of sediment erosion over 15 meters and depth variation ofthe river was 10 to 40 meters. The shallow depth is under the Tenggarong Bridge (10m). In addition, on Line04 shows the deepest depth of the Mahakam River is 35 meters, located in the middle of Line04 or the center of Mahakam river flow.

https://doi.org/10.1088/1755-1315/279/1/012040

OPEN ACCESS 012041
Seismic Hazard Measurement of Earthquake Swarms Activity Based on Horizontal Vertical to Spectral Ratio Analysis (HVSR) in West Halmahera, Indonesia
R W Ningrum, H Fauzi, W Suryanto and E T W Mei
+ Open abstract View article PDF

Identification of eroded sediment layer thickness and depth of Mahakam River at Tenggarong Bridge Area, Kutai Kartanegara East Kalimantan using Ground Penetrating Radar Method

S Rasimeng [1,2*], I Mandang [3] Suharno[1]

[1] Geophysics Engineering Department, University of Lampung, Lampung, Indonesia
[2] Doctoral Programme of Environmental Sciences, University of Lampung, Lampung, Indonesia
[3] Department of Physics, Mulawarman University, Samarinda, Indonesia
*syamsurijal.rasimeng@eng.unila.ac.id

Abstract. GPR measurements of lines are two lines intersect under the bridge of Tenggarong (southwest to northeast) along the 377 meters (segment-1 Line04) and 457 meters (Line03) and the other is Southeast to Northwest along the 533 meters (segment-2 Line04) with a starting point It is located on the side of the Mahakam River (Southern) to the West of Kumala island. and there is one track in this area, which is to the northeast to the southwest along the south side of the Mahakam River (Line02) with the length of line is 780 meters. This research used the AKULA-9000C, 100 MHz antenna frequencies, and in time mode. The purpose of this research is to know the depth of the bottom of the Mahakam River, and the thickness of sediments eroded around the bridge of Tenggarong. GPR data processing using the ReflexW software ver. 8.5 through static correction, subtract-mean (dewow) filter, gain, background removal, band-pass filters, and fk-filter. To convert two-way time of electromagnetic wave propagation data to depth units, we use velocity adaptation methods by selecting velocity value each layer anomaly. Cross sections of the line from line02 and Line03 showed that the average thickness of the layer of sediment erosion over 15 meters and depth variation of the river was 10 to 40 meters. The shallow depth is under the Tenggarong Bridge (10m). In addition, on Line04 shows the deepest depth of the Mahakam River is 35 meters, located in the middle of Line04 or the center of Mahakam river flow.

Keywords: Mahakam, GPR, Tenggarong bridge, riverbed.

1. Introduction

The Mahakam River has a flow system that passes through Kutai Barat, Kutai Kartanegara, and Samarinda City, and the Mahakam upstream in West Kutai flows to the Mahakam delta, with estuaries in the Makassar Straits. Some notes explain that the Mahakam River is the second longest river in Indonesia with a length of 920 km. Mahakam River is widely used by humans as an important transportation route in the area of Samarinda City and Kutai Kartanegara Regency, so the Mahakam River falls into the class of priority river based on the Republic of Indonesia Presidential Decree Number 12 of 2012 about the Determination of River Areas.

The silting of the Mahakam River caused by the soil layer which eroded by rainwater and turned through the tributaries into the Mahakam river flow. In addition, the overhaul of the soil layer by coal mining activities also contributes to sedimentation on the Mahakam river. Both processes are the impact of the high sedimentation process on the Mahakam river. In 2009 to 2013 the Mahakam watershed lost 128,000 hectares of natural forest due to mining activities, HTI, forest concession rights and plantations. Until 2013, the Mahakam watershed left only 4.1 million hectares of natural forest or 50% of total area of the watershed. Conversion of the function forest to non-forest is increasingly uncontrollable. Moreover, there will be more overlapping use of the area between corporations on the same land. East Kalimantan province has lost 112 ha of forest each year [1].

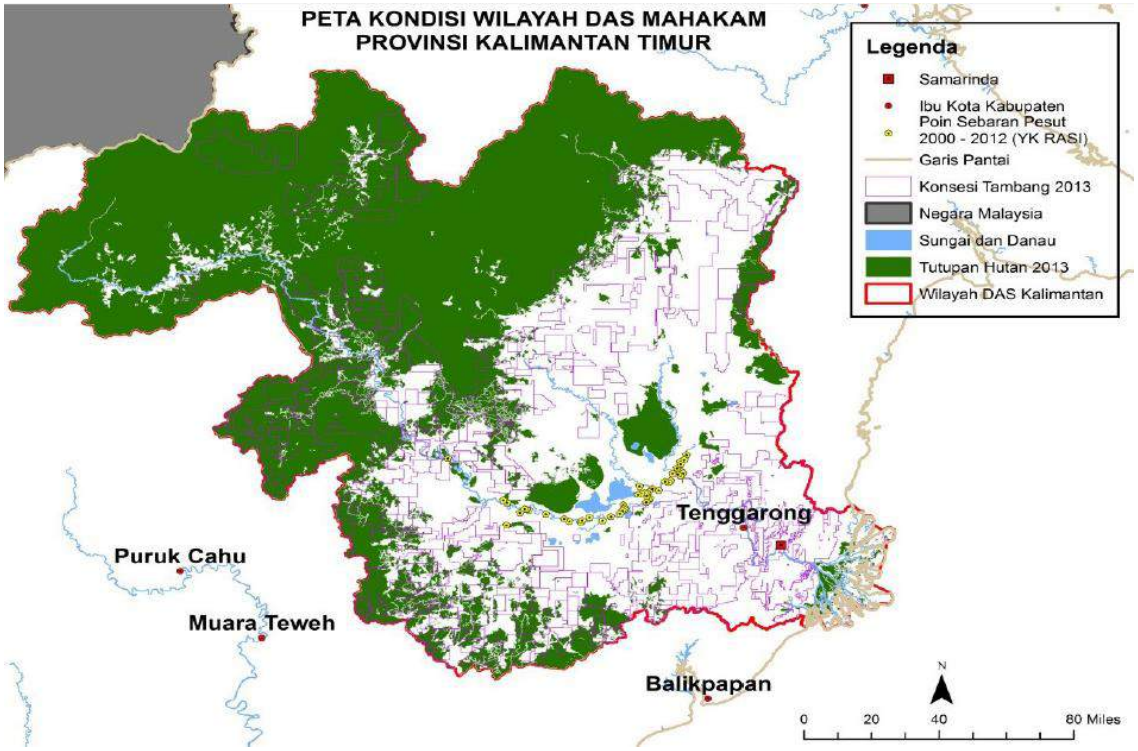

Figure 1. Mahakam watershed and the surrounding environment [1].

Formation of Mahakam delta since Quaternary period was strongly influenced by the mixing of fluvial sedimentation transport processes and influence tidal currents [2, 3, 4] to form fan morphology in transition environment low energy. The stratigraphy of Mahakam delta from Late Plistocene to recent shows continuation of gradation process starting from sea level decline, first rise up to the modern phase/highstand [5]. Interaction between river flow, ocean waves and the slight influence of low to medium energy sequences forming "lobately" of Mahakam delta was drained by river canals and tidal canals. Mahakam delta morphology characterized by absence of alluvial floods, deposits of alluvial levees, fluvial overbank, and splay deposits in delta plain which is a distinguishing feature of the Mahakam Delta with other fluvial-dominated deltas [2].

Vegetation of deltas Mahakam consists of nipa palm and mangrove forests and other primary forests with almost 80% has undergone a conversion process and the remaining only 15 to 20% (22,000 to 30,000 ha). Land use changes have led to an increase rate sedimentation (4 to 10 million tons/year, followed by high abrasion process (139 ha/year) [6]. These evidences indicate the high dissolved soil material along the Mahakam river flow.

These evidences indicate the high dissolved soil material along Mahakam river flow. Sediment analysis is often used as an environmental indicator such as sedimentary texture to find sediment deposition and transport environments [7, 8], sediment grain size to decide sedimentary processes [9], minerals in sediments to determine the origin of sediment sources/rock [9].

The GPR methods are a geophysical technique non-destructive investigation for detecting and identifying subsurface structures to guide decision making of engineer by increasing knowledge about subsurface features, both of natural or artificial. In the civil structures case, the scientific literature only reports several cases of GPR applications for detecting cavities and discontinuities in hydraulic resilience structures such as river embankments and embankment systems [32]. GPR techniques have been used for a century for developing military, detect tunnels and stockpile mines [10]. Currently, GPR applied in various technical surveys for mapping of subsoil features. Some literature reports many applications that documented GPR to at some practical problems like following cases,

- Utility locations: drains, sewer and storm channels, electricity, telephone, cable TV, etc. [11].
- Concrete detection: localization of reinforcement and metal channels, measurement of rebar radius, slab thickness and other property detection [12, 13, 15].
- Monitoring bridges and trains [14].
- Road checks: analysis of pavement structures [16].
- Geological investigations: bedrock profiles, fracture mapping, sedimentology [18, 19].
- Environmental studies and underground hydrogeophysical studies: storage tank locations, soil contamination, mapping water tables, groundwater content [20, 21, 22]

In recent years, investigations of civil structures have improved and supported by national and international standards [32]. However, the literature for application of GPR techniques for river bed sedimentation monitoring is still limited. Identification of sediment layer thickness on the river bed is important information for predicting sediment deposition rates and river shipping safety, so that river water overflows and disruption of vessel traffic can be prevented in river transportation.

2. Methodology

GPR method is one of the geophysical methods for subsurface mapping in shallow layers. Measurement of GPR data can be displayed in real time, so it is possible to assess the quality of data obtained directly in the field. Another advantage of the GPR method is the ability to record data continuously over large areas in a relatively short time. This is helpful because parameter adjustments and quick acquisition arrangements can be made. The basic principle of the GPR method is recording high frequency electromagnetic waves produced by the boundaries of subsurface layers and rocks, based on the reflector response it is possible to detect the dielectric characteristics of existing soil layers [32]. In other words, the response shown contrasts effect of dielectric permittivity on the boundaries of layers and targets buried in subsurface.

The variation of dielectric permittivity contrast value is directly proportional to the contrast of reflectivity coefficient variation. Where the value is related to changes in texture, lithology, porosity and density including water content in the soil layer. Water content also affects the amount of absorption of electromagnetic energy which causes a decrease in wave energy. The difference in soil moisture content can produce a relative dielectric permittivity surge.

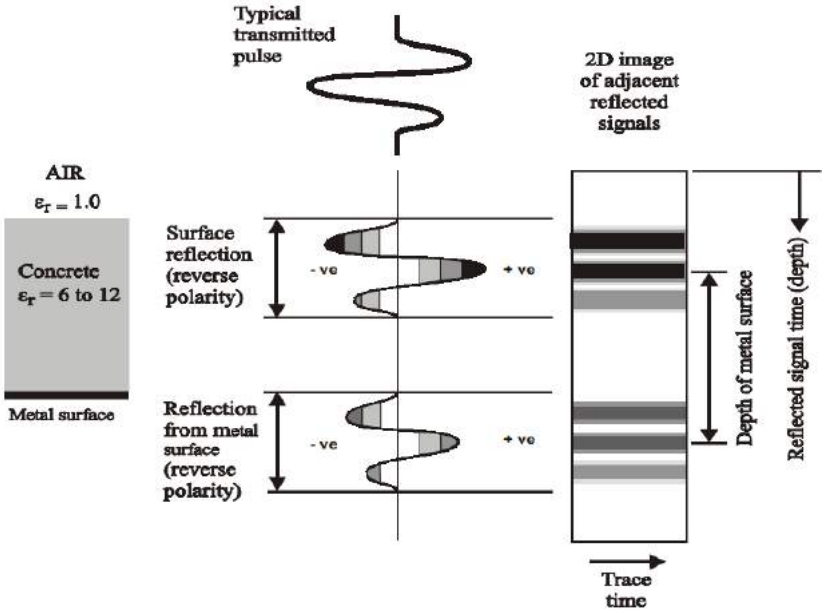

Figure 2. Schematic of radar signal reflection [15].

Source of electromagnetic waves generated from GPR transmitters and transmitted through an antenna, emits pulses with a certain frequency, and spreads in the subsurface have a velocity propagation depending on the medium of the soil layer being passed. When a wave transmitted through a medium that has different dielectric properties, then some of the energy will be reflected and partially transmitted to a deeper layer of soil. Two important dielectric parameters that influence the propagation characteristics of electromagnetic waves in the reflector are conductivity and relative dielectric permittivity [32],

$$\sigma = \frac{1}{\rho} \tag{1}$$

$$\varepsilon_r = \frac{\varepsilon_b}{\varepsilon_o} \tag{2}$$

where σ is conductivity (1/Ωm), ρ is resistivity (Ωm), ε_r is permittivity of material (F/m) and ε_o is permittivity of the vacuum (ε_o = 8.85 10^{-12} F/m) and ε_b is porous media can be considered as the sum of ε_r of different phases,

$$\varepsilon^{\alpha} = \theta_l \varepsilon_l^{\alpha} + \theta_a \varepsilon_a^{\alpha} + \theta_s \varepsilon_s^{\alpha} \tag{3}$$

where ε_l, ε_a, and ε_s are the permittivity of the dielectric of water, air and solid phase. α is a geometric parameter (usually equal to 0.5) which depends on the position of the ineral particles. θ_l, θ_a, and θ_s are the volumetric fractions of each phase. This relationship is called a dielectric mixture model [23]. Seen in Table (1) water has the highest ε_r value which can be used as an indication to determine the layer with a large water content.

Table 1. Conductivity (σ) relative dielectric permittivity (εr) and velocity (v) reference values for common land and rocks [32].

Material	$\mathcal{E}_r$	σ (1/ohm.m)	v(m/ns)
Air	1	0	0.3
Distilled water	80	0.01	0.033
Water	80	0.5	0.033
Marine water	80	0.003	0.01
Dry sand	3-5	0.01	0.15
Wet sand	20-30	0.1-1	0.06
Limestone	4-8	0.5-2	0.12
Shale	5-15	1-100	0.09
Silt	5-30	1-100	0.07
Clay	5-40	2-1000	0.06
Granite	4-6	0.01-1	0.13
Dry salt	5-6	0.01-1	0.13
Ice	3-4	0.01	0.16
Frozen ground	3-6	-	-
Concrete	4-10	-	-
Metal	1-2	-	-

The equipment that will use in this study is a set of GPR tools with equipment of; (i) AKULA 9000C main unit (ii) GPR transmitter (iii) receiver (iv) antenna 100 MHz and (v) GPS. In addition, we use software GasXp (acquisition software) GPRSoft and ReflexW (processing and modeling software). All equipment, laptops and software used are available at Geophysics Exploration Laboratory and Geophysical Data Processing and Modeling Laboratories, Geophysical Engineering Department, Faculty of Engineering, University of Lampung.

The GPR method or commonly called the geo-radar methods, comes from two words: geo means earth and radar (radio detection and ranging). Literally, it means the earth tracking device use radio waves. The component of GPR method for measuring subsurface conditions usually consists of control unit, transmitter antenna and receiver. The transmitter and receiver antenna modes on the GPR consist of mono-static and bi-static modes. Mono-static mode is when the transmitter and receiver combination in one antenna so that there is no distance between transmitters and receiver, while bi-static mode if the two antennas were separation distance [24].

The transmitter generates EM wave pulses at certain frequencies according to characteristics of the antenna (10 MHz to 1000 MHz). The receiver is set to do a scan that normally manages 32 to 512 scans/second. Each scan result is displayed on the PC (real time) as a time function as two-way time, in time needed for EM wave to propagate from transmitters, target and to the receiver is called radar-gram. Principle of GPR tool is transmitting radar waves into the medium by the antenna and then reflected waves to surface and received by radar receiver from reflection wave in response various kinds of objects and recorded in radar-gram. A mechanism of GPR and the example of radar-gram recording are shown in the following figure (2),

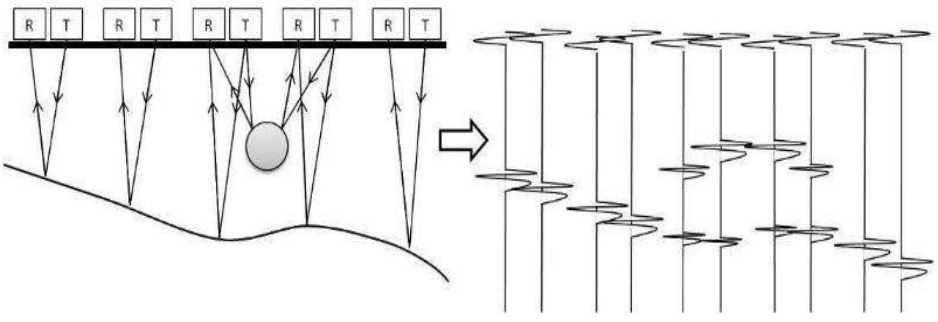

Figure 3. Illustration of how a radargram is generated.

Transmitter and receiver are transducers that convert electric current to EM waves and the antenna transmit electromagnetic waves to propagate to the subsurface. Currently GPR equipment generally records data digitally, making it easier to process data. Digital control of GPR system consisting of a micro-processor, memory and storage for storing field measurement data. In addition, GPR equipment is also equipped with a microcomputer, a standard operating system and an interface to control the process of measuring and storing data by the operator.

GPR data is taken along the path and simultaneously recorded on the hard drive. When radar waves encounter structural continuity (a drastic difference in material properties), a portion of the wave will be reflected and will be in the form of a secondary impulse. The Impulse is then captured by the receiver's antenna and then recorded as observation data, and if the data is interpreted correctly, then the data will show the subsurface structure of the object/material being observed. When the data is taken continuously in horizontal scale on radar-gram is determined by speed of movement of the antenna. Vertical scale is the depth recording interval which is set at frequency sampling. Recording interval presents maximum two-way travel time recorded. The GPR travel time is then converted into depth by calibrating the known object in it or by performing a common midpoint stack with a bi-static antenna around the flat reflector and separating the transmitter and receiver.

Response of radar system relates to the filter of the transmitter antenna, receiver and target response is related with reflection of subsurface objects. GPR penetration capability depends on signal frequency, antenna radiation efficiency and material dielectric properties. Radar signals with high frequencies will produce higher resolutions with limited depth, whereas low-frequency radar signals will produce a deep penetration depth but the resolution is low [25]. The radar wave frequency emitted can be adjusted by changing the antenna. Antenna dimensions vary with radar wave frequency, for example; 1 GHz antenna measuring 30 cm while 25 MHz antenna has a length of 6 m, frequency used depends on the size of the target, approximation of the depth range and maximum aperture of penetration depth.

GPR investigation consists of measuring wave propagation time based on the reflection of conductive rock layers below the surface. Based on the mechanical wave velocity approach v (m/s) with a path along L (m), the position of the reflected field can be determined [11] based on the equation,

$$v = \frac{2L}{t} \tag{4}$$

where t is the time (s).

Equation (4) describes reflected waves for surveys using bi-static antennas. For GPR signals that are affected by the separation between receivers and transmitter (offset) [26] the speed is,

$$v = \frac{c}{\sqrt{\mu_r \varepsilon_r}} \tag{5}$$

where c is the speed of light in a vacuum of 3.10^8 m/s, $\mu = \mu_r \mu_o$ is magnetic permittivity ($\mu_o = 4\pi.10^{-7}$ V/Am), ε_r is dielectric permittivity relative.

In the GPR survey, the depth of the subsurface layer obtained is not exact, but depends on reducing the wave energy that passes through the subsurface medium. Several factors that influence the weakening of electromagnetic waves in the GPR method include; high conductivity of medium, water content, presence of clay minerals, salt content in soil and antenna frequency. The depth interval ranges from 0.40 to 120 m especially for highly conductive medium, whereas in non-conductive medium it can reach 80 m [27]. The vertical resolution of a GPR cross section is the ability to distinguish two reflectors vertically and is usually called type A scanning [10]. According to Nyquist rule, the distance X in ideal conditions equal to 0.25λ, but in reality X is greater than half of the wavelength. Therefore, the selection of antenna frequency values depends on the target anomaly to be detected by considering the high resolution and depth of investigation [32].

3. Analysis and Discussion

GPR investigation for clay layer sometimes presents its own difficulties due to several processes and double layer polarization or spatial polarization [29, 30, 31]. The polarization effect occurs at different frequencies causes dielectric permittivity, and electrical conductivity will be increased, and energy dissipation and weakening reflection. In addition, clay is usually associated with concentration of dissolved ions through ground water, which causes a large absorption of electromagnetic waves energy [28, 29].

Field measurement data processing is carried out based on stages; (i) Static Correction, (ii) substract-mean (dewow), (iii). Background removal, (iv) band-pass filter, (v) time to depth conversion. The other stages, FK-filter, automatic gain, resampling trace, equidistance trace, fk-migration, picking and mingration. The following is the final results of the GPR cross section in the distance depth region.
Profile Line-02

Figure 4. Location of profile Line02 (MHK21).

The Line02 trajectory with the Northeast to Southwestern direction is located south of Kumala Island, Tenggarong, with a line length of 780 meters. Interpretation of GPR cross sections based on; (i) the continuity of the dominant reflector on each measurement path, (ii) the difference in reflection patterns and (iii) the difference in amplitude between the reflectors [17].

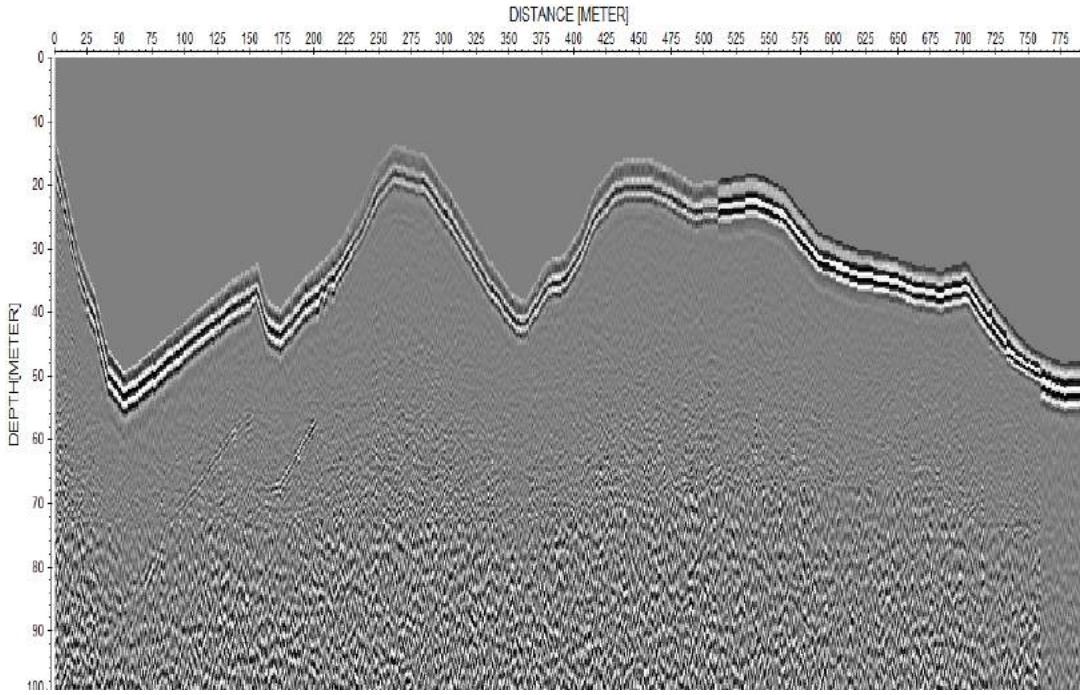

Figure 5. Cross-section of radar-gram profile Line02.

Line02 shows a varied undulation pattern of Mahakam river bed, the depth its 15 to 50 meters with shallow depth at a distance of 275 meters from the starting point of the track. The shallow depth of Line02 is interpreted as a result of the influence of sedimentation from the land. This can be seen from the changes in river banks that are relatively protruding into the river. The other shallow depths are at a distance of 450m which also strongly influenced by the pattern of river banks jutting towards to the river. The thickness of river bed sediment layer around 5 to 10 meters which is a eroded from land and has not compacting, this can be seen from amplitude pattern. Under the sediment layers are estimated as a more compact sediment layer.

Profile Line-03

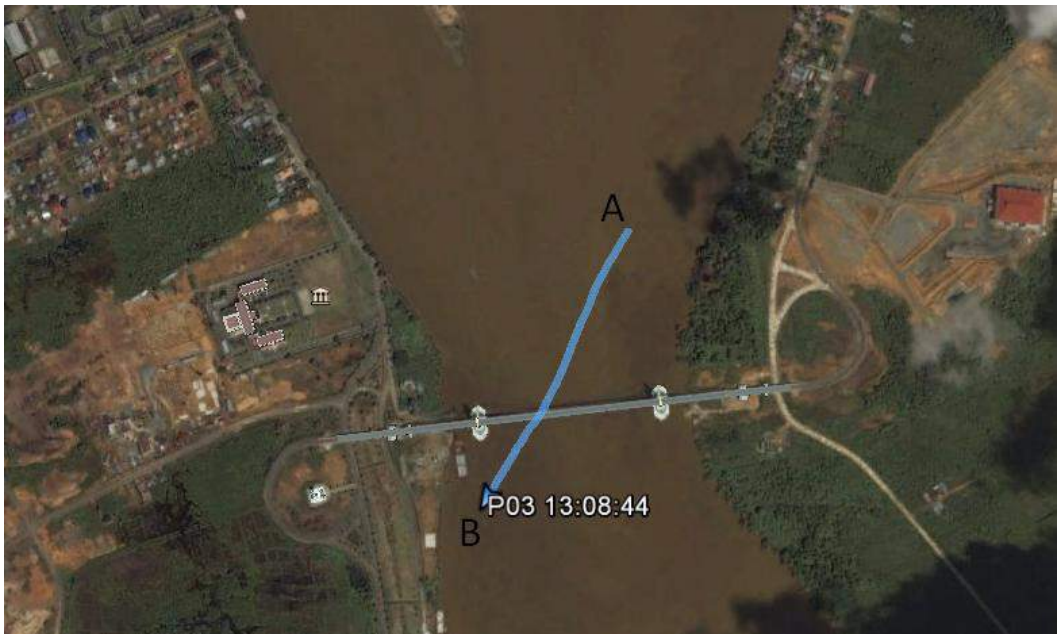

Figure 6. Location of profile Line03 (P03).

Line03 with relatively direction at Northeast to Southwestern is located on the west of Kumala Island Tenggarong and intersects with Tenggarong Bridge, with a measurement line of 450 meters.

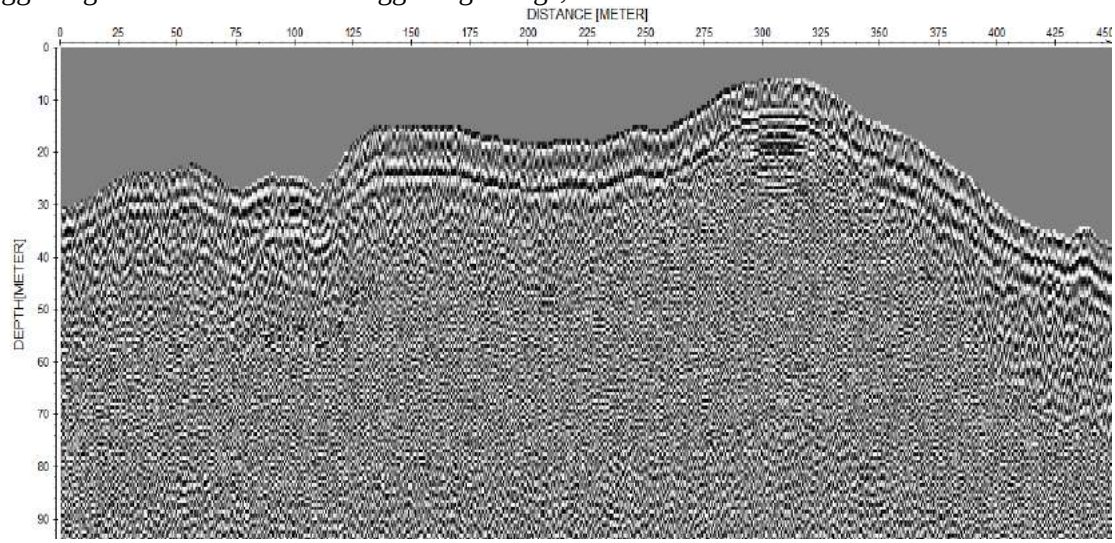

Figure 6. Cross-section of radar-gram profile Line03

The content of organic matter in sediment layer is a sign that there is a limit to the sediment sequence. Whereas non-sedimentary rock layers can be identified based on dielectric contrast values in the GPR cross section. [11]. Line03 shows that the undulation pattern of the Mahakam river bed is relatively stable. The depth of river bed between 5 to 40 meters, with a sludge sediment thickness of more than 20 meters. Location of shallow depth point of Mahakam river bed at 280 to 325 meters from the starting point of line03, exactly below the Tenggarong Bridge. In addition, anomalies around this location are seen in lenses form at radar-gram. The existence of anomaly lens was interpreted as part of the Tenggarong bridge material which collapsed in 2011. The silting of Mahakam river bed around Tenggarong Bridge was caused by the accumulation of sedimentary material due to obstruction of the debris from collapsed bridge. Below the sediment layers are estimated to be a basement rock layer.

Profile Line-04

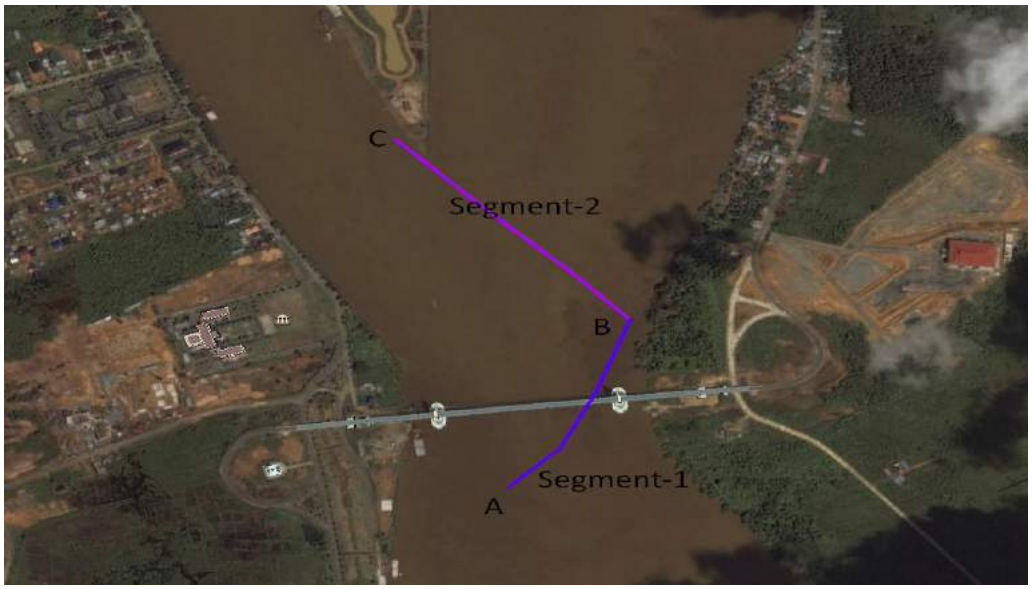

Figure 7. Location of profile Line04.

Location of Line04; Southwest to Northeast direction (segment-1: 0 to 375 meter) and Southeast to Northwest direction (Segment-2: 375 to 535 meter) so that the total length is 910 meters. This line intersects Tenggarong Bridge in segment-1, and segment-2 intersects of Mahakam River the end at the western edge of Kumala Island.

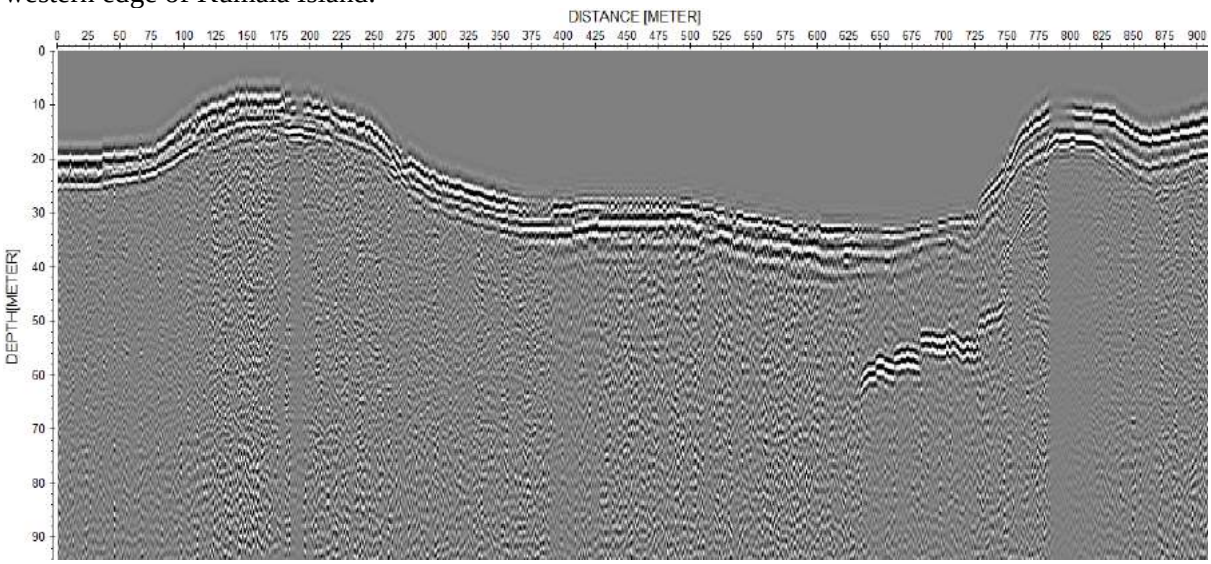

Figure 8. Cross-section of radar-gram profile Line04.

Line04 shows that the undulation pattern of the Mahakam river bed is relatively stable. The depth of river bed between 7 to 30 meters, where shallow depths are at a distance of 130 to 225 meters from starting point of lines. The shallow depth of this line below Tenggarong Bridge. This siltation is probably caused by obstruction of sediment material carried by water flow of the Mahakam river debris, because this path is in line with Mahakam river flow.

The presence of the Mahakam river debris is seen from the Mahakam river bed reflector pattern just below continuous Tenggarong Bridge. Besides that the emergence of anomalous patterns just below the river bed sediment layer. The thickness of sediment layer of river bed is more than 10 meters which is a sediment from soil overhaul and has not undergone compaction. This can be seen from the amplitude pattern. Below the sediment layers are estimated as a more compact sediment layer.

4. Conclusion and Discussion

Based on the results of the GPR cross section analysis, it was concluded that,

a. Undulation pattern of Mahakam river bed that varies with a depth of 15 to 50 meters (Line02); between 7 and 40 meter (Line03); between 7 and 30 meter (Line 04).
b. The shallow depth from 2D GPR section is interpreted due to influence of sedimentation from the land and obstruction of sediment material carried over by the remnants of the Mahakam river debris.
c. The thickness of the river bed sediment layer around 5 to 10 meters which a sediment resulting from errored land and has not compacting.
d. Further search is needed to determine the Mahakam river sedimentation rate.
e. Cross checking of chemical sediment content is needed, to determine the basic sediment materials at the river bed.

References

[1] Forest Watch Indonesia 2016 *Intip Hutan Indonesia: Menyelamatkan Hutan, Menyelematkan Bumi* http://fwi.or.id/ (access on Oct 25th, 2018).
[2] Allen G P, Mercier F 1994 *Proc. of the Indonesian Petroleum Association* p. 261-273.

[3] Lambert B 2003 Micropaleontological investigations in the modern Mahakam delta, East Kalimantan (Indonesia) *Carnets de Géologie/Notebooks on Geology–Article* 2003/02 (CG2003_A02_BL).
[4] Husein S, Lambiase J J 2005 *Proc. of the Indonesian Petroleum Association* p. 367-379.
[5] Roberts H H and Sydow J 1996 *Proc. of the Indonesian Petroleum Association Twenty-Fifth Silver Anniversary Convention* p. 147-161.
[6] Hidayati D, Yogaswara H, Djohan E 2006 *Partisipasi Stakeholders Dalam Konsolidasi Tanah Delta Mahakam: Alternatif Penataan Kawasan* (unpublished).
[7] Sambuelli L, Calzoni C, Pesenti M 2009 *GEOPHYSICS* **74** (4) pp. B95-B104.
[8] McLaren P 1981 *Journal of Sedimentary Petrology* **51** pp. 611-624.
[9] Pettijohn F J 1975 *Sedimentary Rocks*, 3rd ed., Harper and Row, Publishers, Inc. New York, Evanston, San fransisco, and London, pp. 628.
[10] Daniels D J 2004 *Ground Penetrating Radar* 2nd Edition, IET.
[11] Brito G L M, Coutinho A P, Cabral J J S P, Neto S M S, Antonino A C D, Cirilo J A, Braga R A P, Filho S L S 2018 *Revista Brasileira de Recursos Hídricos Brazilian Journal of Water Resources*.
[12] Bungey J H 2004 *Constr Build Mater* **18** pp. 1–8.
[13] Barrile V, Paccinotti R 2005 *NDT&E Int* **38** pp. 596–604.
[14] Chang C W, Lin C H, Lien H S 2009 *Constr Build Mater* **23** pp. 1057–1063.
[15] Sukma A M, Krisningrum N N, Assyiffa T N, Alami F, Rasimeng S, Alhadi A 2018 Ground penetrating radar (GPR) for identifying the depth of spun pile gas station at Batam *The 43rd Annual Scientific Meeting of Indonesian Geophysicists Association* Semarang.
[16] Evans R, Frost M, Stonecliffe-Jones M, Dixon N 2006 *Proc Inst Civ Eng Munic Eng* **159** (2) 105–111.
[17] Emanuel Huber and Peter Huggenberger 2016 *Hydrol Earth Syst Sci* **20** pp. 2035-2046.
[18] Beres M, Haeni F P 1991 *Ground Water* **29** 375–386.
[19] Neal A 2004 *Earth-Sci Rev* **66** 261–330.
[20] Mellet J S 1995 *Appl Geophys* **33** 157–166.
[21] Pyke K, Eyuboglu S, Daniels J J, Vendl M 2008 *J Environ Eng Geophys* **13** 335–342.
[22] Gerhards H, Wollschläger U, Yu Q, Schiwek P, Pan X, Roth K 2008 *Geophysics* **73** (4) J15–J23.
[23] Birchak J R, Gardner C, Hipp J E, Victor J M 1974 Proc. IEEE **62** 93–98.
[24] Akula 2018 *9000 Radar Control Units* www.geoscanners.com. Sweden.
[25] Arcone S A, Finnegan D, Laatsch J E 2006 Bathymetric and subbottom surveying in shallow and conductive water: *Proc. of the 11th International Conference on Ground Penetrating Radar*.
[26] Huisman J A, Hubbard S S, Redman J D, Annan A P 2003 *Vadose Zone J* **2** 476–491.
[27] Sheng Huoo N, Ching-Kuan C, Hong-Ming L 2002 Application of ground penetrating radar on the void-detection in levee. *Proc. Int. J. Offshore Polar Eng*.
[28] Saarenketo T 1998 *J Appl Geophys* **40** 73–88.
[29] Ishida T and Makino T 1999 *J Colloid Interface Sci* 212.
[30] Santamarina J C, Klein K A, Fam M A 2001 *Soils and Waves: Particulate Materials Behavior, Characterization and Process Monitoring* John Wiley and Sons New York.
[31] Bittelli M, Salvatorelli F, Rossi Pisa P 2008 Geoderma 143, pp. 133–142.
[32] Di Prinzio M, Bittelli M, Castellarin A, Pisa P R 2010 *J Appl Geophys* **71** 53–61.

Acknowledgments
We would like to thank for Ministry of Environment, Republic of Indonesia as funding. Thank's to Hydro-Oceanography Team, Department of Physics, Faculty of Mathematics and Natural Science, Mulawarman University for the GPR acquisition team. Thank's to Geophysics Exploration Laboratory and Geophysical Data Processing and Modeling Laboratory, Department of Geophysical Engineering, University of Lampung for equipment and software supporting.